Remote Sensing of Environment 157 (2015) 35–47

Contents lists available at ScienceDirect

Remote Sensing of Environment

journal homepage: www.elsevier.com/locate/rse

Distinguishing surface cyanobacterial blooms and aquatic macrophytes using Landsat/TM and ETM + shortwave infrared bands

Yoichi Oyama *, Bunkei Matsushita, Takehiko Fukushima

Faculty of Life and Environmental Sciences, University of Tsukuba, 1-1-1 Tennoudai, Tsukuba, Ibaraki, 305-8572, Japan

ARTICLE INFO

Article history:
Received 30 December 2013
Received in revised form 26 March 2014
Accepted 17 April 2014
Available online 4 July 2014

Keywords:
Landsat
Inland water
Cyanobacteria
Aquatic macrophytes
SWIR bands

ABSTRACT

Satellite remote sensing can be considered a suitable approach to monitor the extent of cyanobacterial blooms compared with conventional ship surveys because of the patchiness and high spatial and temporal variability of the blooms. However, most of the existing algorithms are not capable of distinguishing cyanobacterial blooms and aquatic macrophytes due to their similar spectral characteristics in the red and near infrared (NIR) wavelengths. In this study, we conducted in situ spectral measurements and satellite data analyses for cyanobacterial blooms and aquatic macrophytes to find an effective method to distinguish them using medium-resolution Landsat satellite images. The reflectance spectra were measured for lake waters and cyanobacterial blooms with 13 different chlorophyll-a concentration levels (from 54 to 21,736 μg L^{-1}) and four types of aquatic macrophytes (two emerged and two floating-leaved macrophytes) in the wavelength range from 350 to 2500 nm. In addition, seven Landsat images were collected for nine lakes in Japan or Indonesia. We calculated several selected indices, i.e., the normalized difference vegetation index (NDVI), five types of normalized difference water index (NDWI), and the floating algal index (FAI) to find an appropriate index for distinguishing cyanobacterial blooms and aquatic macrophytes.

The results showed that the spectral characteristics of cyanobacterial blooms were significantly different from those of aquatic macrophytes in the short-wave infrared (SWIR) region, indicating that the SWIR bands are important for distinguishing cyanobacterial blooms and aquatic macrophytes. The results also showed that the combination of FAI and $NDWI_{4,5}$ was an effective method for classifying lake areas. We first used the FAI for extracting lake waters, and we then used the $NDWI_{4,5}$ to classify the remaining areas as cyanobacterial blooms or aquatic macrophytes. The results also showed that the threshold of $NDWI_{4,5}$ was less sensitive to the effects of both the atmosphere and mixed pixels compared to the other indices. Our application of the FAI threshold of 0.05 and the $NDWI_{4,5}$ threshold of 0.63 to six lakes in Japan and Indonesia showed that the proposed method could successfully distinguish lake water, cyanobacterial blooms, and aquatic macrophytes.

1. Introduction

Cyanobacterial blooms are one of the most serious problems in inland waters due to their negative effects on human activities. Increased turbidity due to a cyanobacterial bloom causes the deterioration of water quality for drinking, agricultural, and industrial uses (Klapper, 1991). An unfavorable appearance or unpleasant odor due to the bloom is a nuisance that affects recreational activities such as boating and swimming (Dodds et al., 2009). In addition, cyanobacterial toxins (cyanotoxins) have become a concern for human health and animal poisoning (Codd, 2000). Cyanobacterial blooms have a great impact on aquatic environments, including reduced transparency, elevated pH, and oxygen depletion (Carpenter et al., 1998; Havens, 2007). These effects also influence the community structure and biodiversity of aquatic flora and fauna. For example, oxygen depletion can preclude fish and other biota (e.g., macroinvertebrate) from the hypolimnion and bottom sediments, bringing about changes in their taxonomic structure (Havens, 2007).

In many lakes, the presence of aquatic macrophytes is another concern. Invasion by mats of free-floating plants is an important threat to the function and biodiversity of freshwater ecosystems (Janse & Van Puijenbroek, 1998). Dark, anoxic conditions under a thick floating macrophyte cover can cause tremendous damage to animals and plants (Scheffer & Van Nes, 2007). In tropical lakes, the water hyacinth (*Eichhornia crassipes*) has dramatic negative impacts on fisheries and boat traffic (Gopal, 1987; Mehra, Farago, Banerjee, & Cordes, 1999).

Since the early 1970s, satellite remote sensing has been widely used to monitor the cyanobacterial blooms (e.g., Kahru, Leppänen, & Rud, 1993; Kahru, Savchuk, & Elmgren, 2007; Kutser, Metsamaa, Strömbeck, & Vahtmäe, 2006; Subramaniam, Brown, Hood, Carpenter, & Capone, 2002). A valuable tool, satellite remote sensing obtains more reliable information about the extent of cyanobacterial blooms compared to conventional ship survey because of their patchiness and

* Corresponding author. Tel./fax: +81 29 853 7189.
E-mail address: y-oyama@ies.life.tsukuba.ac.jp (Y. Oyama).

http://dx.doi.org/10.1016/j.rse.2014.04.031
0034-4257/

high spatial and temporal variability (Kutser, 2004). Several indices for monitoring algal blooms (e.g., diatom, dinoflagellate, and cyanobacterial blooms) have been suggested, such as the maximum chlorophyll index (MCI; Gower, King, Borstad, & Brown, 2005), the cyanobacteria index (CI; Wynne et al., 2008), the maximum peak height (MPH) algorithm (Matthews, Bernard, & Robertson, 2012) and the floating algal index (FAI; Hu, 2009). These indices were developed based on a linear baseline algorithm, relying on three bands (one band corresponds to the reflectance peak often present in the red to near-infrared (NIR) region, and the other two bands are one shorter and one longer than the wavelength of the first band; Gower, 1980; Letelier & Abbott, 1996).

The MCI, CI, and MPH algorithm can be used with a medium-resolution imaging spectrometer (MERIS), and are calculated from the combination of red and NIR bands with the narrow wavelength range; for example, band 8 (677.5–685.0 nm), band 9 (700.0–710.0 nm), and band 10 (750.0–757.5 nm). In contrast, the FAI was developed for used with a moderate-resolution imaging spectroradiometer (MODIS) based on the red, NIR and short-wave infrared (SWIR) bands with broad wavelength ranges; i.e., band 1 (620–670 nm), band 2 (841–876 nm) and band 5 (1230–1250 nm). This band combination can be also applied to many medium-resolution satellite sensors (e.g., Landsat/TM, ETM + and OLI; EO-1/ALI; Terra/ASTER; SPOT/HRVIR and HRG; and ResourceSat/LISS-III), which makes it possible to monitor small lakes and ponds at low cost.

One problem with the FAI is that it is unable to distinguish cyanobacterial blooms and aquatic macrophytes. This is because they have similar spectral characteristics around the NIR region (Dekker et al., 2001; Gower et al., 2005) and thus show similar FAI values. Although the wavelength around 620 nm, which has a absorption peak due to phycocyanin (a specific photosynthetic pigment in cyanobacteria), could be used to distinguish cyanobacterial blooms from aquatic macrophytes (e.g. Dash et al., 2011; Dekker, Malthus, & Goddijn, 1992; Simis, Peters, & Gons, 2005; Tyler et al., 2009), only a few satellite sensors such as MERIS, OCM (Ocean Colour Monitor) and hyperspectral sensors (e.g., Hyperion and CHRIS (Compact High Resolution Imaging Spectrometer)) provide this band, and thus this absorption peak cannot be used with a multispectral satellite sensor. On the other hand, although Landsat-style imaging has only limited spectral bands, it has an advantage over sensors like MERIS because of its high spatial resolution, and making it useful for mapping small-scale features.

The objectives of the present study were: (1) to understand the spectral characteristics of cyanobacterial blooms and aquatic macrophytes by comparing their in situ reflectance measurements; (2) to propose an effective method to distinguish cyanobacterial blooms and aquatic macrophytes using medium-resolution Landsat satellite sensors; and (3) to test the proposed method using Landsat/TM and ETM + images obtained in different periods and lakes.

2. Methods

2.1. In situ data collection

Field investigations were carried out on August 2 and 3, 2012 in three Japanese lakes (Lakes Kasumigaura, Inba-numa and Tega-numa; Fig. 1). In this period, cyanobacterial blooms (mainly *Mycrocystis* spp.) were observed in the western part of Lake Kasumigaura. The waters with different chlorophyll-a (Chl-a) concentrations in the lake are shown in Fig. 2a–e. Here, we defined 'cyanobacterial bloom' as a state the cyanobacteria had begun to accumulate at the water surface (Fig. 2b–e).

We measured reflectance spectra at 13 water areas with different levels of Chl-a concentration in Lake Kasumigaura (10 for cyanobacterial blooms and three for lake waters). The reflectance spectra for cyanobacterial blooms with high aggregations were measured from the shore of Lake Kasumigaura.

Water samples were taken immediately after the spectral measurements, using a clear cylinder sampler (15-cm diameter, 50-cm length). The cylinder sampler was slowly lowered into the water to minimize the disturbance to the cyanobacterial blooms. The sampling volume was kept constant (from the surface to 20 cm deep) at all stations because the concentration of cyanobacteria can be easily changed with the sampling volume when the cyanobacteria are aggregating on the water surface.

The water samples were brought back to the laboratory and then used for the Chl-a measurements by a spectrophotometric method. An amount of particles was collected by filtering the water sample onto a Whatman GF/F glass-fiber filter (47-mm diameter, 0.7-mm pore size). Methanol (100%) was used to extract Chl-a, and the extract was incubated at 4 °C for 24 h in the dark. The extract was then centrifuged at 3000 rpm for 5 min and analyzed with a spectrophotometer (UV-1600, Shimadzu, Kyoto, Japan). The optical density (OD) of the chlorophyll extract was measured at four wavelengths: 750, 663, 645 and 630 nm, and Chl-a concentrations were calculated using SCOR-UNESCO equations (SCOR-UNESCO, 1966).

We also measured the reflectance spectra for two emerged macrophytes (*Nelumbo nucifera* and *Phragmites communis*) in Lake Tega-numa and two floating-leaved macrophytes (*Nymphoides peltata* and *Trapa natans*) in Lakes Kasumigaura and Inba-numa, respectively (Fig. 2f–i). Spectral measurements were conducted using a FieldSpec FR spectroradiometer (Analytical Spectral Devices, Boulder, CO) with the wavelength range from 350 to 2500 nm. We conducted the measurements of the upwelling radiance (L_u) (W m^{-2} sr^{-1}) ten times at the same station, and we used the averaged radiance values for the reflectance calculation. We measured the downwelling radiances (L_d) using a Spectralon reflectance panel (12.5 cm × 12.5 cm, Labsphere, Reflectance Calibration Laboratory, North Sutton, NH) before and after the upwelling radiance measurements, and these values were also averaged for the reflectance calculation by the following equation:

$$R(\lambda)=\frac{L_u(\lambda)}{L_d(\lambda)}\times Cal(\lambda) \quad (1)$$

where R is the reflectance, λ is the wavelength, and Cal is the calibration coefficient of the reflectance panel. We ignored the skylight effects for the reflectance calculation in Eq. (1) because our main purpose was to compare the relative relation between reflectances of cyanobacterial blooms and those of aquatic macrophytes. In addition, since the sky conditions were clear and the wind speeds were low (less than 1 m s^{-1}) during the field surveys, the skylight would have had little effect on the measured reflectances (Mobley, 1999). The spectral reflectances were recalculated to Landsat/TM reflectances using the following equation:

$$R_{Bi}=\frac{\sum_m^n (L_u(\lambda)\times SRF_{\mathrm{Bi}}(\lambda))}{\sum_m^n (L_d(\lambda)\times SRF_{\mathrm{Bi}}(\lambda))} \quad (2)$$

where Bi is the TM ith band, SRF is the spectral response function for each TM band, and m and n are the start and end wavelengths of the SRF for each TM band, respectively.

2.2. Satellite data collection

We collected seven Landsat/TM and ETM + images for nine lakes as training and validation data. The nine lakes include five Japanese lakes and four Indonesian lakes (Table 1). Heavy *Microcystis* blooms were observed during the image acquisition periods for Lakes Suwa, Sutami, and Maninjau (Park, Yokoyama, & Okino, 2003; UNESCO/IHP, 2005). In contrast, floating-leaved macrophytes (*T. natans*) have been highly

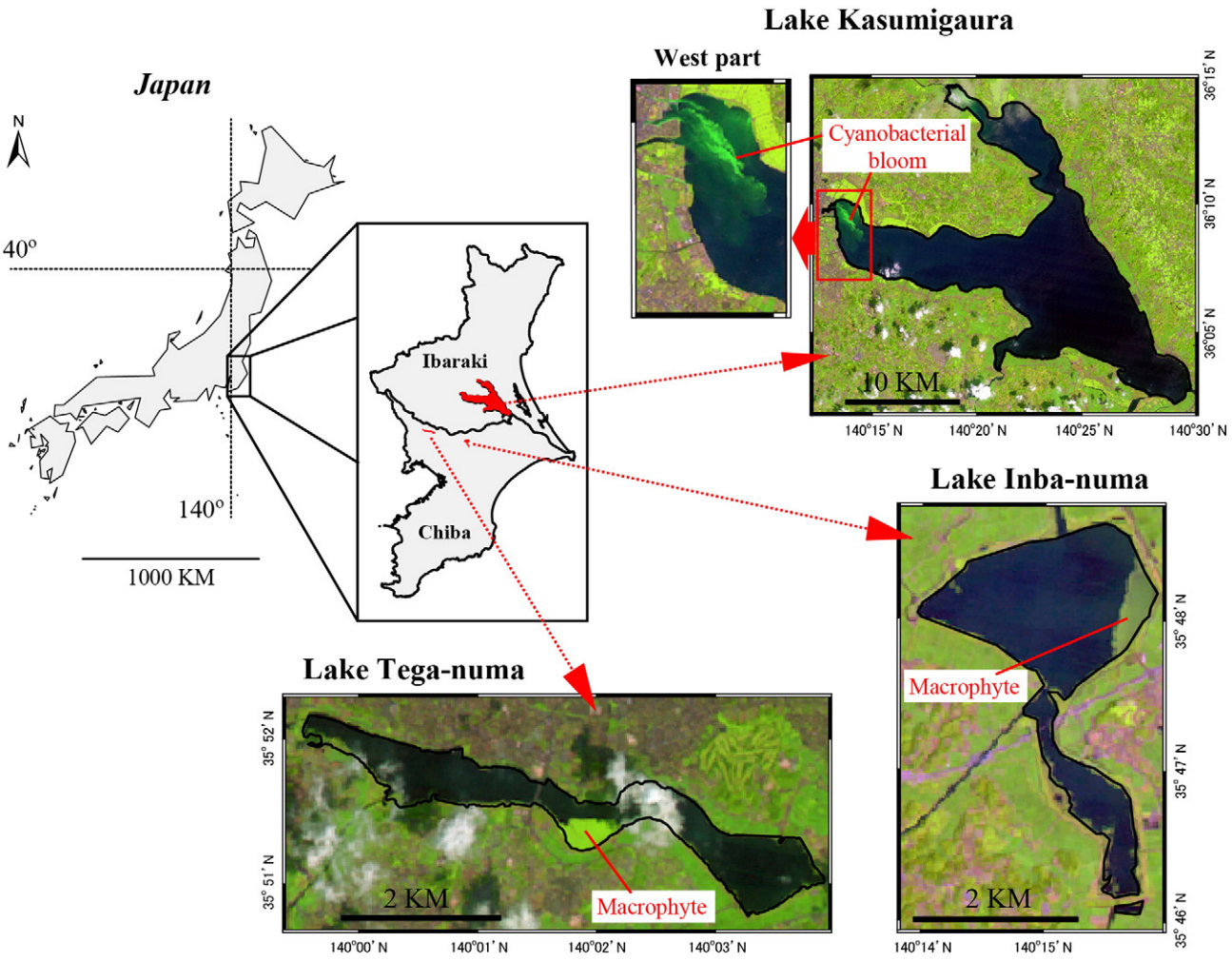

Fig. 1. The locations of Lakes Kasumiguara, Inba-numa and Tega-muma. The Landsat/TM false color images (blue: TM 3, green: TM 4, red: TM 5) on August 11, 2011 are also shown. On this day, cyanobacterial blooms were observed in the west part of Lake Kasumigaura, whereas aquatic macrophytes were found in Lakes Inba-numa and Tega-numa.

distributed in Lakes Mikata and Shirarutoro since the middle of the 2000s (Fukui Prefecture, 2013; Igarashi et al., 2009), and an invasion of water hyacinth (*E. crassipes*) has been a concerned in Lake Limboto since the 1990s (Trisakti & Nugroho, 2012).

The TM sensor has four bands in visible and NIR wavelengths (TM 1: 450–520 nm, TM 2: 520–600 nm, TM 3: 630 — 690 nm, and TM 4: 760 — 900 nm), two bands in SWIR wavelengths (TM 5: 1550–1570 nm, TM 7: 2080 — 2350 nm), and one band in the thermal infrared wavelength (TM 6: 10,400–12,500 nm). The ETM + sensor has the same band configuration except that it includes an additional broad band between 520 nm and 900 nm. The 30-m spatial resolution of TM and ETM + for the multi-bands is required to monitor small inland waters.

The digital numbers (*DN*s) of TM and ETM + were first converted to radiance (*L*) using the following equation:

$$L_{\mathrm{Bi}} = DN_{\mathrm{Bi}} \times \frac{\left(L_{\mathrm{max,\ Bi}} - L_{\mathrm{min,Bj}}\right)}{\left(Qcal_{\mathrm{max,Bi}} + Qcal_{\mathrm{min,Bi}}\right)} - L_{\mathrm{min,Bi}} \tag{3}$$

where L_{max} and L_{min} represent the dynamic range of the TM sensor, and $Qcal_{\mathrm{max}}$ and $Qcal_{\mathrm{min}}$ represent the maximum and minimum quantized calibrated pixel values (typically 255 and 1, respectively for TM). The radiance values were then converted to top-of-atmosphere (TOA) reflectance (R_{TOA}):

$$R_{\mathrm{TOA,Bi}} = \frac{\left(\pi \times L_{\mathrm{Bi}} \times d^2\right)}{\left(F_{0,\mathrm{Bi}} \times \cos\theta_s\right)} \tag{4}$$

where d represents the earth-sun distance (in astronomical units), F_0 represents the extraterrestrial solar irradiance (W m^{-2}), and θ_s represents the solar zenith angle (in radian). In addition, the Rayleigh scattering effects (mainly due to air molecules) were further corrected from the TOA reflectance using the following equation:

$$R_{\mathrm{rc,\ Bi}} = R_{\mathrm{TOA,\ Bi}} - R_{\mathrm{r,\ Bi}} \tag{5}$$

where R_{r} and R_{rc} are the Rayleigh reflectance and the Rayleigh-corrected reflectance, respectively. The R_{r} was calculated based on a radiative transfer code 6S (Vermote, Tanre, Deuze, Herman, & Morcette, 1997). Here we used the middle latitude summer atmospheric model for the Japanese lakes and the tropical atmospheric model for the Indonesian lakes.

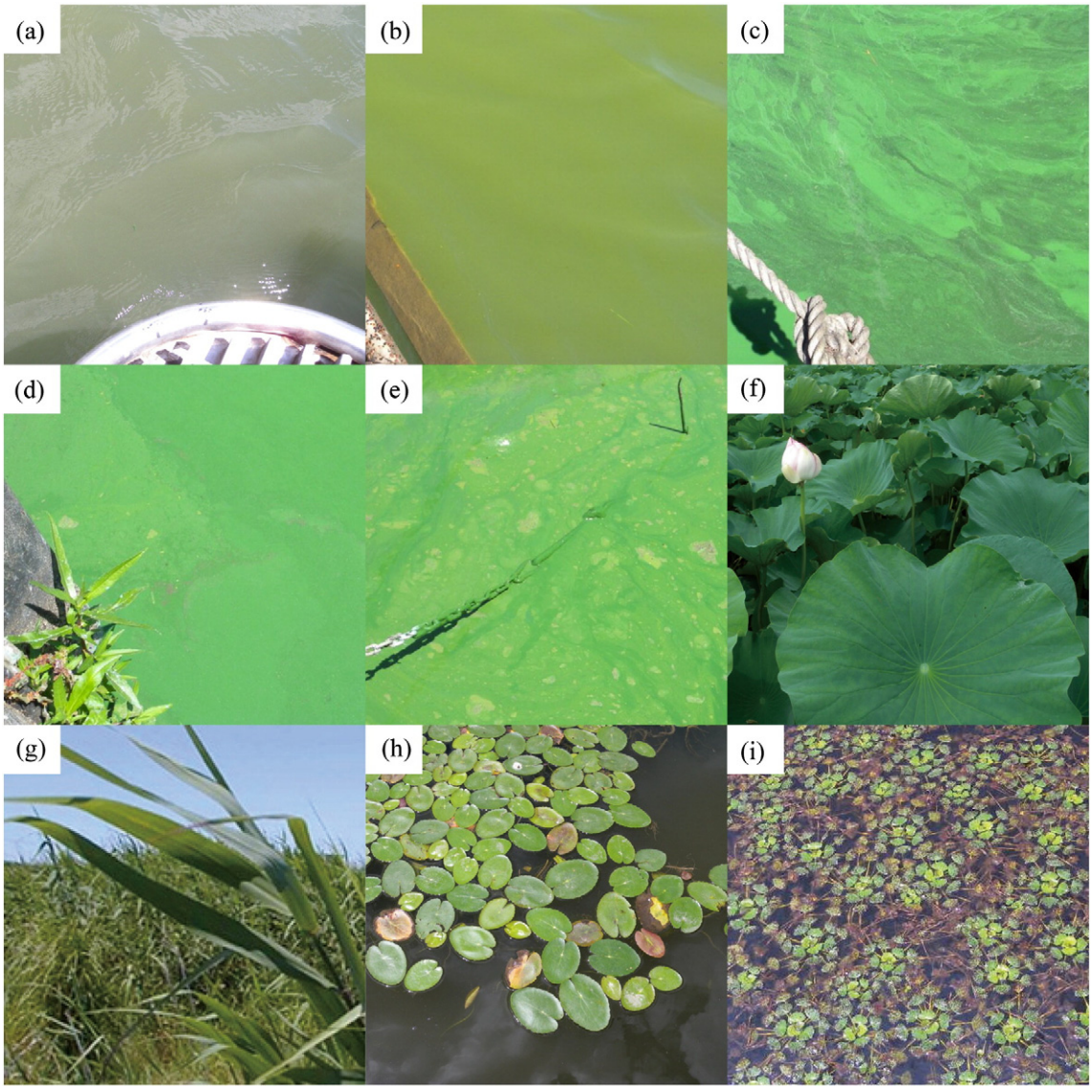

Fig. 2. Photographs of water, cyanobacterial blooms, and aquatic macrophytes observed. (a) Chl-a = 54 μg L^{-1} (lake water), (b) Chl-a = 174 μg L^{-1} (cyanobacterial blooms), (c) Chl-a = 348 μg L^{-1} (cyanobacterial blooms), (d) Chl-a = 2286 μg L^{-1} (cyanobacterial blooms), (e) Chl-a = 21,736 μg L^{-1} (cyanobacterial blooms). (f) *Nelumbo nucifera* (emerged macrophytes), (g) *Phragmites communis* (emerged macrophytes), (h) *Nymphoides peltata* (floating-leaved macrophytes), and (i) *Trapa natans* (floating-leaved macrophytes).

2.3. Selection of indices

We selected several indices that can be calculated from Landsat/TM or ETM + images to distinguish lake water, cyanobacterial blooms, and aquatic macrophytes. The first selected index was the FAI, which was developed to detect cyanobacterical blooms (Hu, 2009). Although the FAI was originally developed for MODIS images, it can also be computed from reflectance in bands 3, 4, and 5 of Landsat/TM or ETM + images using a linear baseline algorithm:

$$\mathrm{FAI} = R_{rc,B4} - \left[R_{rc,B3} + \left(R_{rc,B5} - R_{rc,B3}\right) \times \frac{(\lambda_{B4} - \lambda_{B3})}{(\lambda_{B5} - \lambda_{B3})}\right] \quad (6)$$

Table 1
The seven Landsat images for the nine lakes used in this study.

Target	Location	Date	Path/Row	Sensor	Reference
Cyanobacteria	Lake Kasumigaura (J)	2011/08/11	107/35	TM	This study (training data)
	Lake Suwa (J)	1996/07/14	108/35	TM	Park et al. (2003)
	Lake Sutami (I)	2002/06/04	118/66	ETM+	UNESCO/IHP (2005)
	Lake Maninjau (I)	2000/09/01	127/60	ETM+	UNESCO/IHP (2005)
Macrophyte	Lake Inba-numa (J)	2011/08/11	107/35	TM	This study (training data)
	Lake Tega-numa (J)	2011/08/11	107/35	TM	This study (training data)
	Lake Mikata (J)	2009/08/26	110/35	TM	Fukui Prefecture (2013)
	Lake Shirarutoro (J)	2007/08/02	106/30	TM	Igarashi et al. (2009)
	Lake Limboto (I)	2000/10/17	113/60	ETM+	Trisakti and Nugroho (2012)

(I) Indonesian lake, (J) Japanese lake.

where λ_{Bi} is the center wavelength for the ith band (e.g., $\lambda_{B3} = 660$ nm, $\lambda_{B4} = 830$ nm, and $\lambda_{B5} = 1650$ nm for TM).

The second selected index was the NDVI, which has been widely used for detecting vegetation areas (Rouse, Haas, Schell, & Deering, 1973) and for mapping temporal changes in lake areas (Ma, Wang, Frank, & Dong, 2007) and cyanobacterial blooms (Kahru et al., 1993). The NDVI is calculated as:

$$\mathrm{NDVI} = \frac{(R_{B4} - R_{B3})}{(R_{B4} + R_{B3})}. \quad (7)$$

The third selection was a series of normalized difference water index (NDWI) values, which have been used as a primary tool to enhance water features. For example, McFeeters (1996) proposed an NDWI with the combination of green and NIR bands (corresponding to TM 2 and TM 4, respectively) for distinguishing water and non-water areas; Gao (1996) developed a different NDWI using the combination of NIR and SWIR bands (corresponding to TM 4 and TM 5, respectively) to estimate water content of vegetation; Rogers and Kearney (2004) modified Gao's NDWI by using the red band instead of the NIR band; and Xu (2006) found that the use of a green and SWIR band combination could separate built-up features form water features. In addition to the above four NDWIs, we added another combination (TM 1 and TM 5) for comparison. The general form of NDWI can be written as:

$$\mathrm{NDWI}_{i,j} = \frac{\left(R_{Bi} - R_{Bj}\right)}{\left(R_{Bi} + R_{Bj}\right)} \quad (8)$$

where the subscripts Bi and Bj represent the band numbers used for the NDWI calculation.

2.4. Determination of the threshold for each selected index

The Landsat/TM image acquired on August 11, 2011 was used to determine the threshold for each selected index to distinguish lake water, cyanobacterial blooms, and aquatic macrophytes (Fig. 1). The image covers Lakes Kasumigaura, Inba-numa and Tega-numa. On the same day, cyanobacterial blooms were observed in the western part of Lake Kasumigaura (Ibaraki Prefecture, personal communication). In contrast, only aquatic macrophytes were found in Lakes Inba-numa and Tega-numa by our field survey.

We visually extracted 150 pixels of cyanobacterial blooms from Lake Kasumigaura, a total of 150 pixels of aquatic macrophytes from Lakes Inba-numa and Tega-numa, and a total of 150 pixels of lake waters from the three lakes. We calculated all of the selected indices for the above three groups, and we compared the range of each index for each group to determine whether there were overlaps among the groups. The indices without overlaps between two groups were selected for separating the cyanobacterial blooms and aquatic macrophytes.

The threshold for each index was determined as the average of the maximum and minimum values of two groups. The obtained thresholds were then validated using the remaining six Landsat/TM or ETM+ images for the other six lakes (Table 1).

3. Results

3.1. Spectral features of lake water, cyanobacterial blooms, and aquatic macrophytes

Fig. 3 shows the in situ measured reflectance spectra of the lake water, cyanobacterial blooms, and aquatic macrophytes. Several reflectance spectra correspond to the photos in Fig. 2. The Chl-a concentrations of the lake waters were relatively high (54–144 μg L^{-1}) (Fig. 3a). However, no surface aggregation of cyanobacteria was observed at these sampling stations. The Chl-a concentrations of cyanobacterial blooms varied widely, from 174 to 21,736 μg L^{-1} (Fig. 3b). Blooms with extremely high Chl-a concentrations were also reported by Galat and Verdin (1989) (9790 μg L^{-1}) and El-Alem, Chokmani, Laurion, and El-Adlouni (2012) (>10,000 μg L^{-1}). The reflectance values at the wavelengths ranging from 700 to 1800 nm (i.e., NIR and SWIR regions) were highly increased with the Chl-a concentrations compared to that at visible and wavelengths longer than 1900 nm.

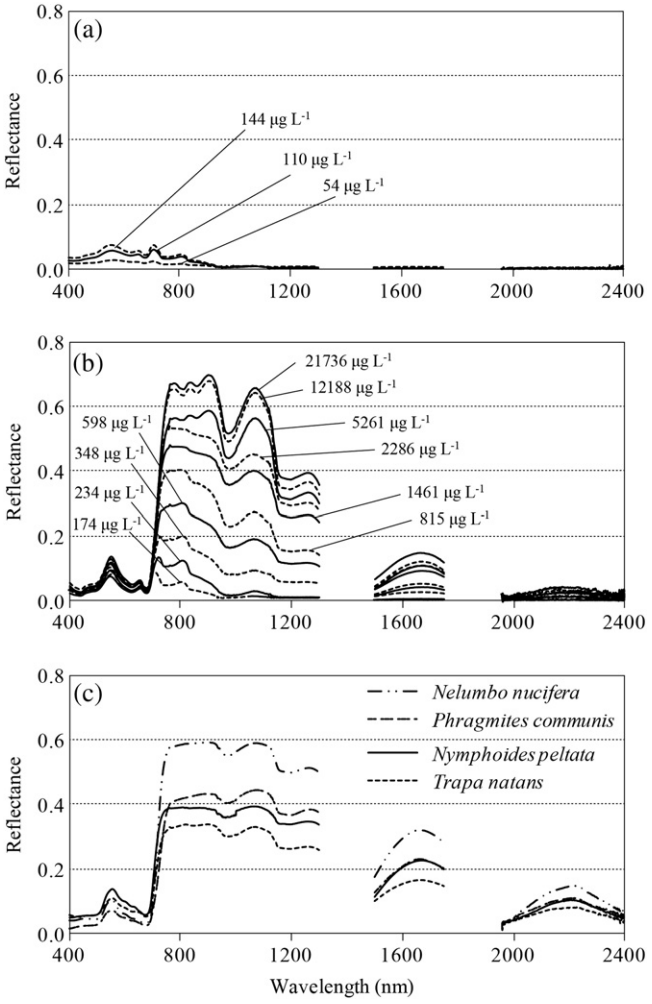

Fig. 3. In situ measured reflectance spectra of (a) lake water, (b) cyanobacterial blooms, and (c) aquatic macrophytes.

In particular, the reflectance values at the NIR region can be higher than 0.6 at the highest Chl-a concentration (21,736 μg L^{-1}) due mainly to the backscatter caused by cyanobacterial cells (Matthews et al., 2012). However, the reflectance spectrum at the Chl-a concentration of 12,118 μg L^{-1} is similar to that at the highest Chl-a concentration, indicating that the reflectances of the heavy cyanobacterial blooms became saturated at these levels of Chl-a. The trough around 620 nm is due to the absorption by the phycocyanin pigment (Dekker et al., 1992). On the other hand, the reflectance spectra of aquatic macrophytes were similar for all investigated species (Fig. 3c).

The reflectance values at the NIR region were much higher than those at the visible region, due mainly to the cellular structure in the leaves (Hoffer, 1978). In addition, the small trough around 970 nm is related to the absorption by water contained in the plants (Peñuelas, Gamon, Griffin, & Field, 1993). This trough was observed not only in the spectra of aquatic macrophytes but also in that of heavy cyanobacterial blooms at high Chl-a concentrations (Fig. 3b–c). It is notable that the SWIR reflectance of the aquatic macrophytes was higher than that of the cyanobacterial blooms.

Table 2
Observed ranges of in situ measured reflectances at each simulated TM band and the selected indices for the groups of lake water, cyanobacterial blooms and aquatic macrophytes.

Index	Range			Distinguishable	
	Lake water	Cyano.[a]	Macrophyte	Lake water and cyano.	Cyano. and macrophyte
TM 1 (450–520 nm)	0.02–0.04	0.02–0.06	0.03–0.06	No	No
TM 2 (520–600 nm)	0.03–0.05	0.05–0.10	0.06–0.11	No	No
TM 3 (630–690 nm)	0.02–0.04	0.03–0.06	0.03–0.07	No	No
TM 4 (760–900 nm)	0.02–0.03	0.04–0.67	0.33–0.58	Yes	No
TM 5 (1550–1750 nm)	0.001–0.004	0.00–0.14	0.16–0.30	No	Yes
TM 7 (2080–2350 nm)	0.001–0.003	0.00–0.04	0.07–0.13	No	Yes
NDVI	−0.22 to −0.21	−0.09–0.85	0.68–0.87	Yes	No
$NDWI_{4,2}$	0.31–0.34	−0.76–0.30	−0.76 to −0.55	Yes	No
$NDWI_{1,5}$	0.81–0.91	−0.45–0.93	−0.77 to −0.46	No	Yes
$NDWI_{2,5}$	0.86–0.93	−0.15–0.96	−0.58 to −0.26	No	Yes
$NDWI_{3,5}$	0.82–0.92	−0.41–0.94	−0.76 to −0.42	No	Yes
$NDWI_{4,5}$	0.74–0.87	0.66–0.93	0.30–0.37	No	Yes
FAI	−0.009 to −0.005	0.00–0.60	0.26–0.50	Yes	No

"Yes" or "No" indicates whether lake water and cyanobacterial blooms were distinguishable, or whether cyanobacterial blooms and aquatic macrophytes were distinguishable.
[a] Cyanobacterial bloom.

3.2. Applicability of the selected indices from in situ data

Table 2 shows the observed ranges of in situ measured reflectances at each simulated TM band and the selected indices for the groups of lake water, cyanobacterial blooms, and aquatic macrophytes. For the single TM bands, the lake water samples show relatively low reflectances for all bands compared to those of the cyanobacterial bloom and aquatic macrophyte samples. We identified overlaps of the ranges of observed reflectance between the lake water and cyanobacterial blooms (except for TM 4), indicating that only the reflectance at the

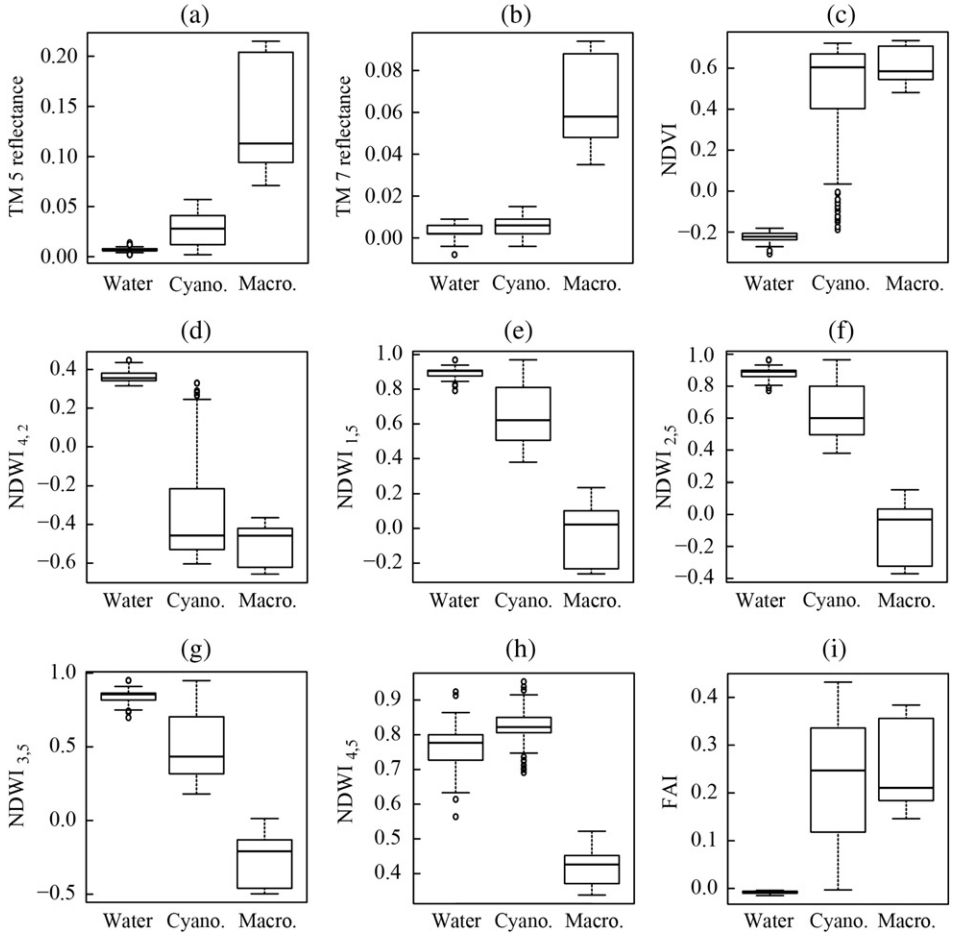

Fig. 4. Box-and-whisker plots of TM reflectances or selected indices for lake water (Water), cyanobacterial blooms (Cyano.) and aquatic macrophytes (Macro.). Each box was calculated from 150 pixels of data extracted from the Landsat/TM image of Lakes Kasumigaura, Inba-numa and Tega-numa on 11 August, 2011 (Fig. 1). The solid line in the box represents the median value. The upper and lower fences represent the 1st and 3rd quartiles (Q1 and Q3), respectively. The lower and upper whiskers were calculated from (Q1 − 1.5 × IQR) and (Q3 + 1.5 × IQR), respectively, where IQR is the interquartile range represented by the width of the box (i.e., Q3 − Q1). The data above or under the whisker were defined as the outliers and are shown as open circles. (a) TM 5 reflectance, (b) TM 7 reflectance, (c) NDVI, (d) $NDWI_{4,2}$, (e) $NDWI_{1,5}$, (f) $NDWI_{2,5}$, (g) $NDWI_{3,5}$, (h) $NDWI_{4,5}$, and (i) FAI.

Table 3
Observed ranges of satellite-derived TM reflectance and selected indices for lake water, cyanobacterial blooms and aquatic macrophytes.

Index	Range			Lake water and cyano.		Cyano. and macrophyte	
	Lake water	Cyano.[a]	Macrophyte	Distinguishable	Threshold	Distinguishable	Threshold
TM 5	0.004–0.010	0.002–0.057	0.071–0.113	No	–	Yes	0.064
TM 7	−0.004–0.009	−0.004–0.015	0.035–0.094	No	–	Yes	0.025
NDVI	−0.27 to −0.18	0.04–0.72	0.48–0.74	Yes	−0.07	No	–
$NDWI_{4,2}$	0.32–0.44	−0.60–0.25	−0.66–0.37	Yes	0.285	No	–
$NDWI_{1,5}$	0.85–0.94	0.38–0.97	−0.26–0.24	No	–	Yes	0.31
$NDWI_{2,5}$	0.81–0.93	0.38–0.97	−0.37–0.15	No	–	Yes	0.27
$NDWI_{3,5}$	0.75–0.91	0.18–0.95	−0.50–0.01	No	–	Yes	0.10
$NDWI_{4,5}$	0.56–0.92	0.75–0.92	0.34–0.51	No	–	Yes	0.63
FAI	−0.015 to −0.004	−0.003–0.432	0.146–0.384	Yes	−0.0035	No	–

The maximum and minimum values in each group were obtained from the upper and lower whisker values in Fig. 4. The thresholds between lake water and cyanobacterial blooms and between cyanobacterial blooms and aquatic macrophytes were calculated from the maximum and minimum values between them. "Yes" or "No" is as explained in Table 2.
[a] Cyanobacterial bloom.

TM 4 band has the potential for separating lake water and cyanobacterial blooms. Similarly, the reflectances at two SWIR bands (TM 5 and TM 7) showed a potential for separating cyanobacterial blooms and aquatic macrophytes.

Among the selected indices, the NDVI, $NDWI_{4,2}$, and FAI showed potential for separating lake water and cyanobacterial blooms, whereas the NDWI with the band combination including the SWIR bands could be used to distinguish cyanobacterial blooms and aquatic macrophytes.

3.3. Applicability of the selected indices from satellite data

We further investigated the applicability of the selected indices for distinguishing lake water, cyanobacterial blooms and aquatic macrophytes using an actual Landsat/TM image (acquired on August 11, 2011, Fig. 1). The results are shown in Fig. 4 and Table 3. The results obtained from two single SWIR bands (TM 5 and TM 7) are also shown for comparison. The TMs 1, 2, 3 and 4 were not used because these bands were not suitable for separation (Table 2). From Fig. 4 and Table 3, it can be seen that the NDVI, $NDWI_{4,2}$ and FAI were effective to separate lake water and others (i.e., cyanobacterial blooms and aquatic macrophytes), but they were less useful for distinguishing cyanobacterial blooms and aquatic macrophytes.

In contrast, the NDWIs calculated from the SWIR and other bands as well as two single SWIR bands showed a significant difference between the cyanobacterial blooms and aquatic macrophytes, indicating a potential for separating them. However, these NDWIs and the two single SWIR bands were not very useful for distinguishing lake water and cyanobacterial blooms. These results indicate that it is necessary to combine the two types of indices for completely separating lake water, cyanobacterical blooms and aquatic macrophytes.

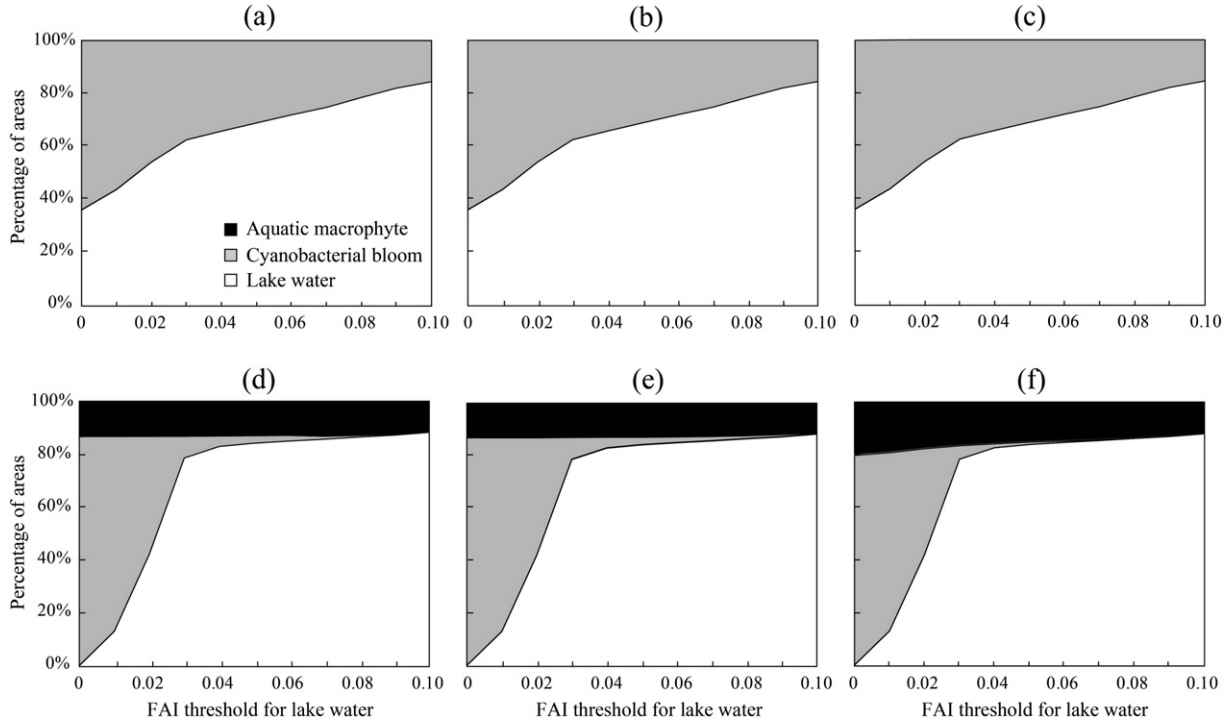

Fig. 5. Changes in the percentage of lake water, cyanobacterial blooms and aquatic macrophytes in two different lakes with varying FAI thresholds for determining the lake water area. The data were obtained from the Landsat/TM images on August 11, 2011 (Fig. 1). a–c: West part of Lake Kasumigaura (cyanobacteria-dominated part). d–f: Lake Inba-numa (macrophyte-distributing lake). These images were first classified into lake water and others (i.e., cyanobacterial blooms or aquatic macrophytes) using FAI thresholds with varying the range from 0 to 0.1 at intervals of 0.01. The other areas were then further classified into cyanobacterial blooms and aquatic macrophytes using the thresholds listed in Table 3. (a, d) TM 7 threshold (0.025), (b, e) $NDWI_{2,5}$ threshold (0.27), and (c, f) $NDWI_{4,5}$ threshold (0.63).

We determined the thresholds for extracting lake waters as well as for distinguishing cyanobacterial blooms and aquatic macrophytes by averaging the maximum and minimum values between the two groups (i.e., lake water and cyanobacterical blooms, and cyanobacterical blooms and aquatic macrophytes; Table 3). The thresholds for extracting lake water were calculated as −0.07 for NDVI, 0.285 for $NDVI_{4,2}$, and −0.0035 for FAI, respectively; the thresholds for distinguishing aquatic macrophytes from cyanobacterial blooms were calculated as 0.064 for TM 5, 0.025 for TM 7, 0.31 for $NDWI_{1,5}$, 0.27 for $NDWI_{2,5}$, 0.10 for $NDWI_{3,5}$, and 0.63 for $NDWI_{4,5}$.

3.4. Redetermination of FAI threshold for extracting lake waters

Since the FAI was specially developed for distinguishing cyanobacterial blooms from lake water (Hu et al., 2010), we employed it for extracting the lake waters in this study even though the NDVI and $NDWI_{4,2}$ could also serve the same purpose. Fig. 5 shows the classification results obtained from the training Landsat/TM image (acquired on August 11, 2011) by using the respective thresholds of TM 7, $NDWI_{2,5}$ and $NDWI_{4,5}$ as well as varied FAI thresholds (from 0 to 0.1 at an intervals of 0.01). We used the FAI to extract lake waters, and we selected the TM 7, $NDWI_{2,5}$ and $NDWI_{4,5}$ to distinguish cyanobacterial blooms and aquatic macrophytes. For the western part of Lake Kasumigaura (heavy cyanobacterial blooms occurred, but no aquatic macrophytes were observed in this test area), no aquatic macrophyte was detected for all FAI thresholds (Fig. 5a–c), indicating that the thresholds of TM 7, $NDWI_{2,5}$ and $NDWI_{4,5}$ were reasonable in this case for distinguishing aquatic macrophytes and others (lake water or cyanobacterial blooms).

However, the area of the detected cyanobacterial blooms changed from 63.8% to 15.5% with the increasing FAI threshold from 0 to 0.1, indicating that the detection of cyanobacterial blooms strongly depends on the determined threshold of FAI. In contrast, for Lake Inba-numa (the lake with aquatic macrophytes distribution), although no cyanobacterial bloom was observed when the Landsat passed over the lake, a large area was detected as cyanobacterial blooms at the low FAI thresholds (Fig. 5d–f). The detected area of aquatic macrophytes did not show a large change for all FAI thresholds. These results also indicate that the detection of cyanobacterial blooms strongly depends on the determined threshold of FAI, and the thresholds of TM 7, $NDWI_{2,5}$ and $NDWI_{4,5}$ are reasonable for distinguishing aquatic macrophytes and others. We therefore adjusted the threshold of FAI to 0.05. At this FAI threshold, the misclassified area as cyanobacterial blooms in Lake Inba-numa was less than 2.8% for TM 7 and $NDWI_{2,5}$ (Fig. 5d, e) and 0.9% for $NDWI_{4,5}$ (Fig. 5f).

3.5. Validations

We applied the determined thresholds for distinguishing lake water, cyanobacterial blooms and aquatic macrophytes to six other Landsat images for six different lakes in Japan or Indonesia (Table 1). The six lakes included three in which cyanobacterial blooms occurred but limited or no aquatic macrophyte distribution was reported. The other three lakes had aquatic macrophyte distributions, but no occurrence of cyanobacterial blooms was reported. The results are shown in Figs. 6 and 7, respectively. The FAI images showed higher values for both cyanobacterial blooms (Fig. 6d–f) and aquatic macrophytes (Fig. 7d–f). The lakes were first separated into lake water and others using the FAI threshold of 0.05. Then, the others were further separated into cyanobacterial blooms and aquatic macrophytes using the thresholds of TM 7 reflectance (0.025), $NDWI_{2,5}$ (0.27) and $NDWI_{4,5}$ (0.63). The classification results by the thresholds of TM 5 reflectance, $NDWI_{1,5}$ and $NDWI_{3,5}$ are not shown because they gave results similar to those obtained with the TM 7 reflectance and $NDWI_{2,5}$.

In the three lakes with cyanobacteria (Fig. 6), the cyanobacterial blooms were successfully detected using the FAI (FAI > 0.05) and thresholds of TM 7 reflectance, $NDWI_{2,5}$ and $NDWI_{4,5}$ in all three lakes. The areas distinguished as aquatic macrophytes were less than 1.5% in two Indonesian lakes (Lakes Sutami and Maninjau). In Lake Suwa, a relatively high distribution of aquatic macrophytes was detected at the south coast of the lake (Fig. 6j, m, p) because this area has been covered by *Trapa* spp. and *Potamogeton* spp. (submerged macrophytes) since the 1980s (Takei, 2004). In contrast, in the lakes with aquatic macrophyte distributions, the aquatic macrophytes were successfully detected by combining the FAI and other indices (TM 7, $NDWI_{2,5}$ and $NDWI_{4,5}$, Fig. 7). Only a few pixels with an FAI larger than 0.05 were misclassified as cyanobacterial blooms (2.1%–15.9% for TM 7, 3.9%–10.3% for $NDWI_{2,5}$, and 0%–0.3% for $NDWI_{4,5}$). The reason for this is discussed in the next section.

4. Discussion

4.1. The importance of the SWIR band for distinguishing cyanobacterial blooms and aquatic macrophytes

In this study we propose the use of $NDWI_{4,5}$ (which uses the NIR and SWIR bands) to distinguish cyanobacterial blooms and aquatic macrophytes on Landsat images. Although the NDWIs have already been proposed by several research groups for delineating water areas or estimating the water moisture of vegetation (Gao, 1996; Rogers & Kearney, 2004; Xu, 2006), the purposes were not for distinguishing cyanobacterial blooms and aquatic macrophytes.

Compared to the aquatic macrophytes, the cyanobacterial blooms showed a deeper trough around 970 nm and lower reflectance at SWIR bands, indicating that the effects of water absorption on cyanobacterial blooms are stronger than those on aquatic macrophytes (Fig. 3). Sridhar and Vincent (2007) also reported the difference of reflectance spectra in SWIR regions between *Microcystis* blooms and duck weeds (floating macrophytes). In addition, since the water absorption in the SWIR band is much stronger than that in the NIR band (Palmer & Williams, 1974), the SWIR band can be considered more effective than the NIR band for distinguishing cyanobacterial blooms and aquatic macrophytes.

To further understand the importance of the SWIR band for distinguishing cyanobacterial blooms and aquatic macrophytes, we carried out a one-way analysis of variance (ANOVA) to compare the between-group variance and the within-group variance using the data shown in Fig. 4 (Table 4). The F-values indicate the significance of differences between the two groups. For example, the F-value of TM 7 is higher than that of TM 5 (1390 vs. 663, respectively), indicating that the difference between cyanobacterial blooms and aquatic macrophytes at TM 7 is more significant than that at TM 5. The results showed that all indices related to the SWIR band have higher F-values; in particular, the $NDWI_{4,5}$ has the highest F-value (6452), indicating that the $NDWI_{4,5}$ is the most effective index for distinguishing cyanobacterial blooms and aquatic macrophytes.

Since TM 7 showed a higher F-value than TM 5, we tested another combination of TM 4 and TM 7 (i.e., $NDWI_{4,7}$). The F-value of $NDWI_{4,7}$ was increased to 7197. However, because of the strong water absorption at TM 7, the reflectance at TM 7 is always low and thus easily influenced by natural 'noise' such as sensor calibration and illumination conditions. We thus do not recommend combinations with TM 7.

4.2. The robustness of the indices for distinguishing cyanobacterial blooms and aquatic macrophytes

4.2.1. Effects of atmosphere

It is necessary to consider the influence of the atmospheric effects such as aerosol scattering and absorption on the NDWIs, because we calculated the NDWIs from the top-of-atmosphere (TOA) reflectance. The use of the TOA reflectance makes it easy to process the satellite data due to the frequent lack of data for atmospheric correction. We

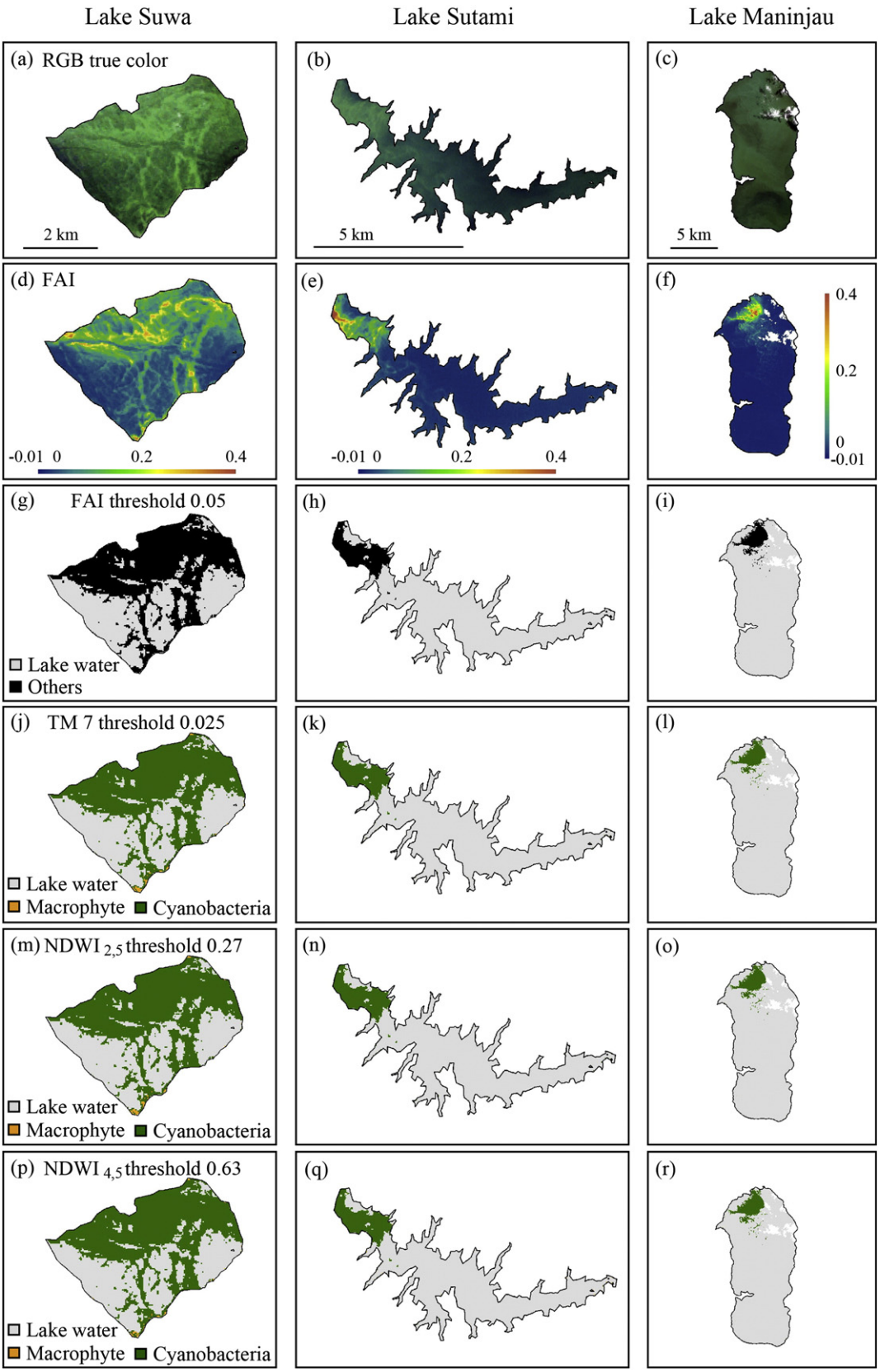

Fig. 6. Landsat images of three lakes in which cyanobacterial blooms occurred but no or small levels of aquatic macrophytes were distributed. a–c: RGB true color images. d–f: FAI images. The images were first separated into lake water and others using the FAI threshold 0.05 (g–i). The others were further separated into cyanobacterial blooms and aquatic macrophytes using the TM 7 threshold of 0.025 (j–l), the $NDWI_{2,5}$ threshold of 0.27 (m–o), and the $NDWI_{4,5}$ threshold of 0.63 (p–r).

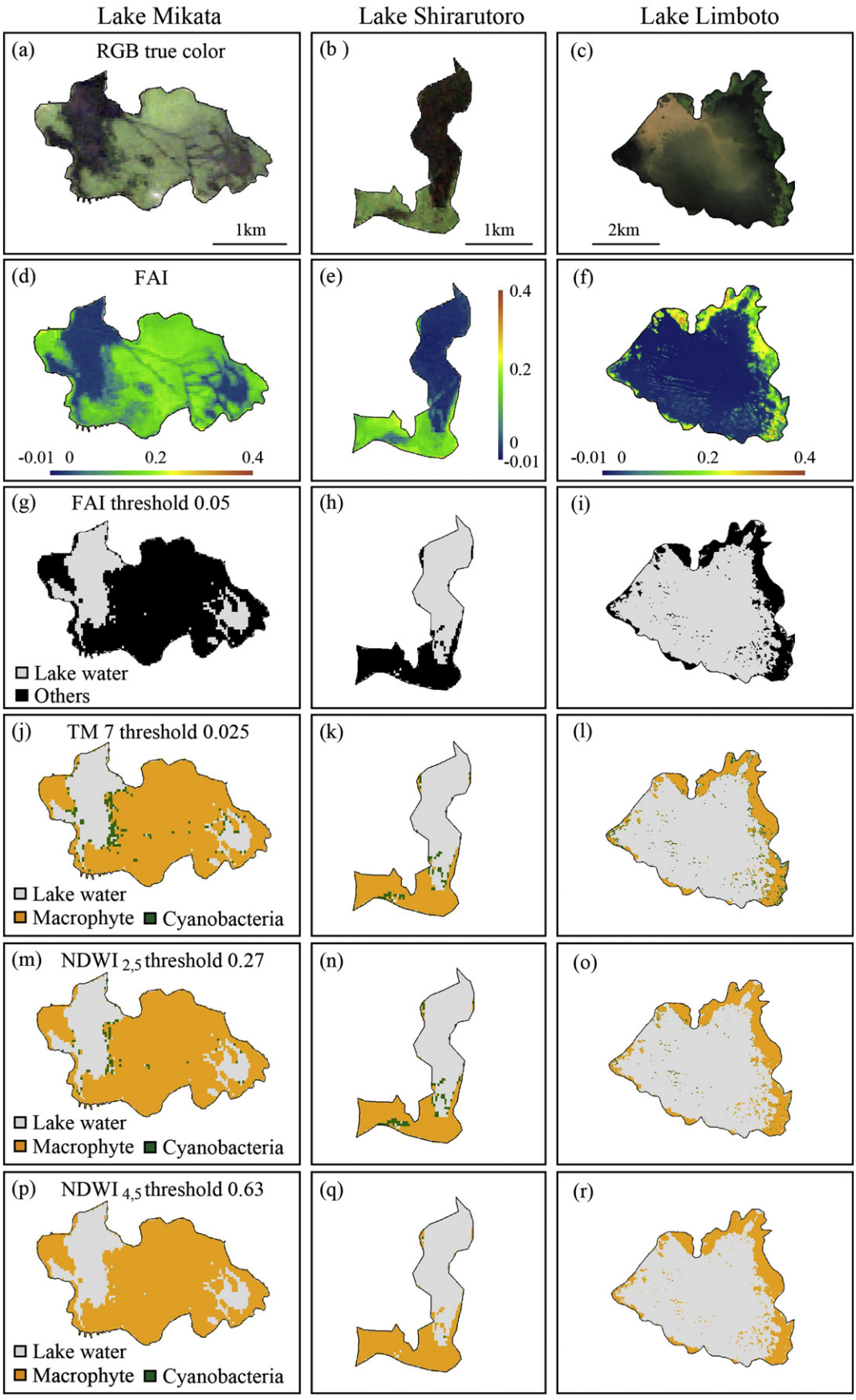

Fig. 7. Similar to Fig. 6 but three lakes where aquatic macrophytes distributed and no occurrence of cyanobacterial blooms.

Table 4
Results of a one-way ANOVA analysis between cyanobacterial blooms and aquatic macrophytes for TM band reflectance and selected indices.

Index	Group	Mean	Variance	Between-group variance	Within-group variance	F-value
TM 1	Cyanobacteria	0.12	0.016×10^{-3}	0.6×10^{-5}	0.024×10^{-3}	0.3
	Macrophyte	0.12	0.032×10^{-3}			
TM 2	Cyanobacteria	0.11	0.035×10^{-3}	0.8×10^{-2}	0.021×10^{-3}	404
	Macrophyte	0.10	0.068×10^{-4}			
TM 3	Cyanobacteria	0.07	0.016×10^{-3}	0.8×10^{-4}	0.011×10^{-3}	7
	Macrophyte	0.07	0.054×10^{-4}			
TM 4	Cyanobacteria	0.28	0.017	0.3	0.013	19
	Macrophyte	0.34	0.009			
TM 5	Cyanobacteria	0.03	0.020×10^{-2}	1.0	0.002	663
	Macrophyte	0.14	0.003			
TM 7	Cyanobacteria	0.01	0.018×10^{-3}	0.3	0.02×10^{-2}	1390
	Macrophyte	0.07	0.036×10^{-2}			
NDVI	Cyanobacteria	0.49	0.068	1.3	0.037	35
	Macrophyte	0.62	0.007			
$NDWI_{4,2}$	Cyanobacteria	−0.33	0.072	2.3	0.041	57
	Macrophyte	−0.51	0.010			
$NDWI_{1,5}$	Cyanobacteria	0.64	0.026	43.6	0.030	1469
	Macrophyte	−0.12	0.033			
$NDWI_{2,5}$	Cyanobacteria	0.65	0.026	36.9	0.027	1370
	Macrophyte	−0.05	0.028			
$NDWI_{3,5}$	Cyanobacteria	0.51	0.046	45.7	0.038	1217
	Macrophyte	−0.28	0.029			
$NDWI_{4,5}$	Cyanobacteria	0.83	0.002	12.6	0.002	6452
	Macrophyte	0.41	0.002			
FAI	Cyanobacteria	0.22	0.017	0.1	0.012	10
	Macrophyte	0.25	0.007			

The data were obtained from Fig. 5.

simulated the influence of the atmosphere on the NDWI thresholds based on the in situ reflectance measurement and 6S code (Vermote et al., 1997). The calculation was performed by varying the aerosol optical thickness (AOT) values from 0 to 1 at intervals of 0.2. We chose the mid-latitude summer model and maritime model for the simulations of atmosphere and aerosol, respectively. We then used the simulated TOA reflectances corresponding to the AOT values to calculate the NDWIs. The results showed that the $NDWI_{4,5}$ was the least sensitive to atmospheric effects, as only 11% changed when the AOT varied from 0 to 1 (Fig. 8). This is because the atmospheric effects in shorter wavelengths are stronger than those in longer wavelengths (Antoine & Morel, 1998).

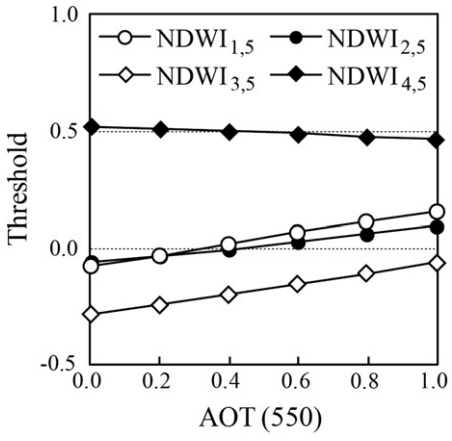

Fig. 8. Changes in the NDWI thresholds between cyanobacterial blooms and aquatic macrophytes with varying aerosol optical thickness (AOT) values for four NDWIs. The NDWI at each AOT value was calculated from simulated TOA reflectances using a 6S radiative transfer algorithm with the in situ measured TM reflectances listed in Table 1.

4.2.2. Effects of mixed pixels

Fig. 7 showed that a few pixels with FAI larger than 0.05 were misclassified as cyanobacterial blooms by the selected indices even though no cyanobacterial bloom occurrences were reported in these lakes. This is probably because these lake pixels were partially covered by aquatic macrophytes. We therefore investigated the influence of mixed pixels on the determined thresholds of NDWIs based on the training data from the Landsat/TM image taken on August 11, 2011 by varying the fraction of aquatic macrophytes from 0% to 100% at intervals of 20% (Fig. 9). The results showed that the $NDWI_{4,5}$ threshold of 0.63 could correctly detect aquatic macrophytes when the fraction of them was larger than 10%. In contrast, the $NDWI_{2,5}$ threshold of 0.27 could only detect aquatic macrophytes if their fractions were larger than 50%. In other words, the aquatic macrophytes would be misclassified as cyanobacterial blooms if the fraction of aquatic macrophytes was less than 50%. This is probably because the TM 4 reflectance has an exponential relationship with the aquatic macrophyte coverage (Jakubauskas, Kindscher, Fraser, Debinski, & Price, 2000). It can thus be proposed that the $NDWI_{4,5}$ is much more robust compared to the other indices.

It is notable that in the case of cyanobacterial blooms and aquatic macrophytes mixed within one pixel, it is difficult to classify the pixel as either of them. Therefore, the proposed method is only suitable for the cases of pixels with the mix of two constituents (i.e., lake water and cyanobacterial blooms, or lake water and macrophytes).

4.3. Threshold of the FAI for extracting lake water

We first used the threshold of the FAI to extract lake water. The definition of lake water strongly depended on the FAI threshold (Fig. 5). A higher FAI threshold will result in the under-detection of cyanobacterial blooms, especially when the blooms have a lower Chl-a concentration, whereas lower FAI thresholds may provide an incorrect warning about an occurrence of cyanobacterial blooms.

The FAI threshold was determined as 0.05 in this study according to the analyses of the training Landsat/TM image (acquired on Aug. 11,

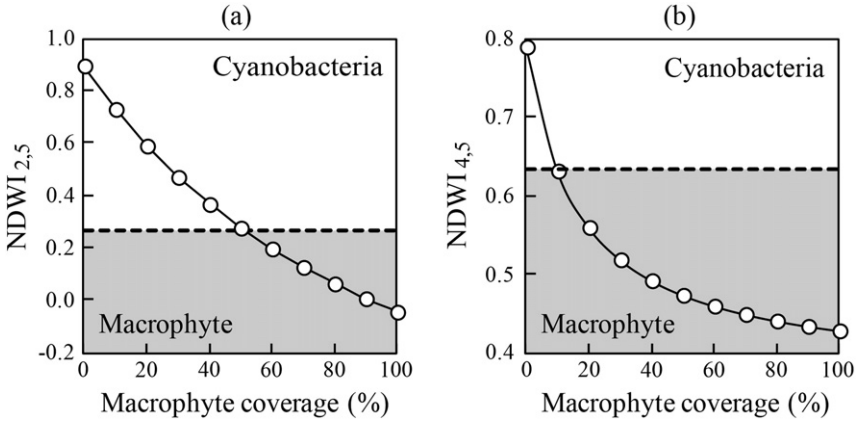

Fig. 9. Changes in the index values with macrophyte coverage. The dotted line represents the threshold between cyanobacterial blooms and aquatic macrophytes (0.27 and 0.63 for $NDWI_{2,5}$ and $NDWI_{4,5}$, respectively; see Table 3). The gray areas represent the area recognized as aquatic macrophytes by the threshold. For the example of $NDWI_{2,5}$, more than 50% of coverage is recognized as macrophytes, whereas the remaining is misclassified as cyanobacterial blooms. The indices were simulated from a simple linear spectral mixture approach using the median value of the lake water and aquatic macrophytes of the Landsat/TM image. (a) $NDWI_{2,5}$ and (b) $NDWI_{4,5}$.

2011) based on our known information. For example, we knew about the occurrence of cyanobacterial blooms in the western part of Lake Kasumigaura but not about any distribution of aquatic macrophytes in the same area and same period, according to personal communication with other researchers. We also knew about the distribution of aquatic macrophytes but no occurrence of cyanobacterial blooms in Lakes Inba-numa and Tega-numa during the same period, according to our field surveys.

Although the validation results reported herein qualitatively showed that the FAI threshold of 0.05 was also appropriate for the other six lakes in Japan and Indonesia, we recommend further validation for determining the most appropriate FAI threshold if the proposed method is used for other lakes, because there are many types of algal and macrophyte communities (e.g., green, red and brown macroalgae) in water areas.

5. Conclusions

In this study, we propose a method to distinguish cyanobacterial blooms and aquatic macrophytes from Landsat/TM and ETM + images by combining the FAI and $NDWI_{4,5}$. We used the FAI first for extracting lake waters, and we then used the $NDWI_{4,5}$ to classify the remaining lake pixels as cyanobacterial blooms or aquatic macrophytes. We found that the threshold of $NDWI_{4,5}$ is less sensitive to the effects of both the atmosphere and mixed pixels compared to other indices. The $NDWI_{4,5}$ threshold of 0.63 and the FAI threshold of 0.05 were qualitatively validated by our use of them for six other lakes in Japan and Indonesia. Further validation is required to test the applicability of these thresholds for other satellite sensors and other regions where different macrophytes and macroalgae are growing.

Acknowledgments

We sincerely thank Dr. Hiroya Yamano and Dr. Akihide Kamei of Japan's National Institute for Environmental Studies (NIES) for the use of the FieldSpec FR spectroradiometer, and the three anonymous reviewers for their helpful comments and suggestions. This research was supported in part by the Global Environment Research Fund (S-9) of Japan's Ministry of the Environment, and by Grants-in-Aid for Scientific Research from Japan's Ministry of Education, Culture, Sports, Science, and Technology (MEXT) (Nos. 23404015 and 25420555).

References

Antoine, D., & Morel, A. (1998). Relative importance of multiple scattering by air molecules and aerosols in forming the atmospheric path radiance in the visible and near-infrared parts of the spectrum. *Applied Optics*, *37*(12), 2245–2259.

Carpenter, S. R., Caraco, N. F., Correll, D. L., Howarth, R. W., Sharpley, A. N., & Smith, V. H. (1998). Nonpoint pollution of surface waters with phosphorus and nitrogen. *Ecological Application*, *8*(3), 559–568.

Codd, G. A. (2000). Cyanobacterial toxins, the perception of water quality, and the prioritization of eutrophication control. *Ecological Engineering*, *16*(1), 51–60.

Dash, P., Walker, N. D., Mishra, D. R., Hu, C., Pinckney, J. L., & D'Sa, E. J. (2011). Estimation of cyanobacterial pigments in a freshwater lake using OCM satellite data. *Remote Sensing of Environment*, *115*(12), 3409–3423.

Dekker, A. G., Brando, V. E., Anstee, J. M., Pinnel, N., Kutser, T., Hoogenboom, E. J., et al. (2001). Imaging spectrometry of water. In F. D. Van der Meer, & S. M. de Jong (Eds.), *Imaging spectrometry: Basic principles and prospective applications* (pp. 307–359). Kluwer Academic Publishers.

Dekker, A. G., Malthus, T. J., & Goddijn, L. M. (1992). Monitoring cyanobacteria in eutrophic waters using airborne imaging spectroscopy and multispectral remote sensing systems. *Proceedings of 6th Australasian Remote Sensing Conference, New Zealand.* , *1*. (pp. 204–214).

Dodds, W. K., Bouska, W. W., Eitzmann, J. L., Pilger, T. J., Pitts, K. L., Riley, A. J., et al. (2009). Eutrophication of U.S. freshwaters: Analysis of potential economic damages. *Environmental Science & Technology*, *43*(1), 12–19.

El-Alem, A., Chokmani, K., Laurion, I., & El-Adlouni, S. E. (2012). Comparative analysis of four models to estimate chlorophyll-a concentration in case-2 waters using moderate resolution imaging spectroradiometer (MODIS) Imagery. *Remote Sensing*, *4*(8), 2373–2400.

Fukui Prefecture (2013). *Implementation planning sheet of nature restoration project in five lakes of Mikata.* , 1–62 (in Japanese).

Galat, D. L., & Verdin, J. P. (1989). Patchiness, collapse and succession of cyanobacterial bloom evaluated by synoptic sampling and remote sensing. *Journal of Plankton Research*, *11*(5), 925–948.

Gao, B. C. (1996). NDWI — a normalized difference water index for remote sensing of vegetation liquid water from space. *Remote Sensing of Environment*, *58*(3), 257–266.

Gopal, B. (1987). *Water hyacinth.* New York: Elsevier.

Gower, J. F. R. (1980). Observations of in situ fluorescence of chlorophyll a in Saanich Inlet. *Boundary-Layer Meteorology*, *18*(3), 235–245.

Gower, J., King, S., Borstad, G., & Brown, G. (2005). Detection of intense plankton blooms using the 709 nm band of the MERIS imaging spectrometer. *International Journal of Remote Sensing*, *26*(9), 2005–2012.

Havens, K. E. (2007). Cyanobacteria blooms: Effects on aquatic ecosystems. In H. K. Hudnell (Ed.), *Proceedings of the Interagency, International Symposium on Cyanobacterial Harmful Algal Blooms (ISOC-HAB): State Of The Science And Research Needs* (pp. 733–747). New York: Springer.

Hoffer, R. M. (1978). Biological and physical considerations in applying computer-aided analysis techniques to remote sensor data. In P. H. Swain, & S. M. Davis (Eds.), *Remote sensing: The quantitative approach* (pp. 227–289). New York: McGraw-Hill.

Hu, C. (2009). A novel ocean color index to detect floating algae in the global oceans. *Remote Sensing of Environment*, *113*(10), 2118–2129.

Hu, C., Lee, Z., Ma, R., Yu, K., Li, D., & Shang, S. (2010). Moderate resolution imaging spectroradiometer (MODIS) observations of cyanobacteria blooms in Taihu Lake, China. *Journal of Geophysical Research*, *115*, http://dx.doi.org/10.1029/2009JC005511.

Igarashi, S., Mikami, H., Ueno, Y., Tanba, S., Nakagawa, K., & Takamura, N. (2009). Distribution of *Trapa Japonica* and plankton in Lake Shirarutoro, Kushiro Mire. *Abstract of 55th Annual Meeting of the Japanese Society of Limnology.* , *62*, (in Japanese).

Jakubauskas, M., Kindscher, K., Fraser, A., Debinski, D., & Price, K. P. (2000). Close-range remote sensing of aquatic macrophyte vegetation cover. *International Journal of Remote Sensing*, *21*(18), 3533–3538.

Janse, J. H., & Van Puijenbroek, P. J. T. M. (1998). Effects of eutrophication in drainage ditches. *Environmental Pollution*, *102*(1), 547–552.

Kahru, M., Leppänen, J. M., & Rud, O. (1993). Cyanobacterial blooms cause heating of the sea surface. *Marine Ecology Progress Series*, *101*, 1–7.

Kahru, M., Savchuk, O. P., & Elmgren, R. (2007). Satellite measurements of cyanobacterial bloom frequency in the Baltic Sea: Interannual and spatial variability. *Marine Ecology Progress Series*, *343*, 15–23.

Klapper, H. (1991). *Control of eutrophication in inland waters*. London: Ellis Horwood.

Kutser, T. (2004). Quantitative detection of chlorophyll in cyanobacterial blooms by satellite remote sensing. *Limnology and Oceanography*, *49*(6), 2179–2189.

Kutser, T., Metsamaa, L., Strömbeck, N., & Vahtmäe, E. (2006). Monitoring cyanobacterial blooms by satellite remote sensing. *Estuarine, Coastal and Shelf Science*, *67*(1–2), 303–312.

Letelier, R. M., & Abbott, M. R. (1996). An analysis of chlorophyll fluorescence algorithms for the moderate resolution imaging spectrometer (MODIS). *Remote Sensing of Environment*, *58*(2), 215–223.

Ma, M., Wang, X., Frank, V., & Dong, L. (2007). Change in area of the Ebinur Lake during the 1998–2005 period. *International Journal of Remote Sensing*, *28*, 5523–5533.

Matthews, M. W., Bernard, S., & Robertson, L. (2012). An algorithm for detecting trophic status (chlorophyll-a), cyanobacterial-dominance, surface scums and floating vegetation in inland and coastal waters. *Remote Sensing of Environment*, *124*, 637–652.

McFeeters, S. K. (1996). The use of the normalized difference water index (NDWI) in the delineation of open water features. *International Journal of Remote Sensing*, *17*(7), 1425–1432.

Mehra, A., Farago, M. E., Banerjee, D. K., & Cordes, K. B. (1999). The water hyacinth: an environmental friend or pest? A review. *Resource Environmental Biotechnology*, *2*, 255–281.

Mobley, C. D. (1999). Estimation of the remote-sensing reflectance from above-surface measurements. *Applied Optics*, *38*, 7442–7455.

Palmer, K. F., & Williams, D. (1974). Optical properties of water in the near infrared. *Journal of the Optical Society of America*, *64*(8), 1107–1110.

Park, H., Yokoyama, A., & Okino, T. (2003). Fate of microcystin in Lake Suwa. *Research Report of the Research and Education Center for Inlandwater Environment Shinshu University.* , *1*. (pp. 79–97) (in Japanese).

Peñuelas, J., Gamon, J. A., Griffin, K. L., & Field, C. B. (1993). Assessing community type, plant biomass, pigment composition, and photosynthetic efficiency of aquatic vegetation from spectral reflectance. *Remote Sensing of Environment*, *46*(2), 110–118.

Rogers, A. S., & Kearney, M. S. (2004). Reducing signature variability in unmixing coastal marsh Thematic Mapper scenes using spectral indices. *International Journal of Remote Sensing*, *25*(12), 2317–2335.

Rouse, J. W., Haas, R. H., Schell, J. A., & Deering, D. W. (1973). Monitoring vegetation systems in the Great Plains with ERTS-1. *3rd Earth Resources Technology Satellite Symposium* (pp. 309–317).

Scheffer, M., & Van Nes, E. H. (2007). Shallow lakes theory revisited: Various alternative regimes driven by climate, nutrients, depth and lake size. *Hydrobiologia*, *584*(1), 455–466.

SCOR-UNESCO (1966). *Determination of photosynthetic pigment in seawater. Monographs on oceanographic methodology*, *1*. (pp. 11–18). Paris: UNESCO, 11–18.

Simis, S. G. H., Peters, S. W. M., & Gons, H. J. (2005). Remote sensing of the cyanobacterial pigment phycocyanin in turbid inland water. *Limnology and Oceanography*, *50*(1), 237–245.

Sridhar, B. B. M., & Vincent, R. K. (2007). Spectral reflectance measurements of a *Microcystis* bloom in Upper Klamath Lake, Oregon. *Journal of Great Lakes Research*, *33*, 279–284.

Subramaniam, A., Brown, C. W., Hood, R. R., Carpenter, E. J., & Capone, D. G. (2002). Detecting *Trichodesmium* blooms in SeaWiFS imagery. *Deep Sea Research, Part II*, *49*(1–3), 107–121.

Takei, K. (2004). Change of distribution of submerged plant *Potamogeton crispus* L. in Lake Suwa. *Bulletin of Nagano Prefectual Fisheries Experimental Station*, 8–13 (in Japanese).

Trisakti, B., & Nugroho, dan-G. (2012). Monitoring the change of lake quality during 1990–2011 using multi temporal satellite image. *Proceeding of Seminar National Limnologi.* , *4*. (pp. 342–351) (in Indonesian).

Tyler, A., Hunter, P. D., Carvalho, L., Codd, G. A., Elliott, J. A., Ferguson, C. A., et al. (2009). Strategies for monitoring and managing mass populations of toxic cyanobacteria in recreational waters: A multi-interdisciplinary approach. *Environmental Health*, *8*, S11.

UNESCO/IHP (2005). CYANONET: A global network for cyanobacterial bloom and toxin risk management, initial situation assessment and recommendations. In G. A. Codd, S. M. F. O. Azevedo, S. N. Bagchi, M. D. Burch, W. W. Carmichael, W. R. Harding, K. Kaya, & H. C. Utkilen (Eds.), *IHP-VI, Technical Document in Hydrology.* , *76*, . Paris: UNESCO.

Vermote, E. F., Tanre, D., Deuze, J. L., Herman, M., & Morcette, J. J. (1997). Second simulation of the satellite signal in the solar spectrum, 6S: An overview. *IEEE Transactions on Geoscience and Remote Sensing*, *35*(3), 675–686.

Wynne, T. T., Stumpf, R. P., Tomlinson, M. C., Warner, R. A., Tester, P. A., Dyble, J., et al. (2008). Relating spectral shape to cyanobacterial blooms in the Laurentian Great Lakes. *International Journal of Remote Sensing*, *29*(12), 3665–3672.

Xu, H. (2006). Modification of normalized difference water index (NDWI) to enhance open water features in remotely sensed imagery. *International Journal of Remote Sensing*, *27*(14), 3025–3033.